**British Journal of Physics Studies**
ISSN: 000-000
DOI: 10.32996/bjps
Journal Homepage: www.al-kindipublisher.com/index.php/bjps

**BJPS**
**AL-KINDI CENTER FOR RESEARCH AND DEVELOPMENT**

**| RESEARCH ARTICLE**

# Polythermal Nucleation Kinetics of $NaHCO_3$-$Na_2CO_3$-$H_2O$ in the Presence of Polyectrolyte Additives

**Caroline Ruth Etroubeka[1], Daniel Asiedu[2] and Isaac D. Tegladza[3]** ✉
*[1]College of Chemistry and Chemical Engineering, Nanjing Tech University, Nanjing, 210009, China*
*[23]College of Chemical Engineering, Nanjing Tech University, Nanjing, 210009, China*
**Corresponding Author:** Isaac D. Tegladza, **E-mail**: 2393902638@qq.com

## | ABSTRACT
The particle size distribution (PSD) of substances is important to their transportation and packaging. The crystal nucleation kinetics measured from the metastable zone width (MSZW) and/or the induction time are vital to the control of the PSD. In this work, the existence of three polyelectrolyte additives (sodium polystyrene sulfonate (SPS), Polyacetic acid (PAA) and sodium carboxymethylcellulose (CMC)) showed varying effects on the MSZW and induction times of $NaHCO_3$-$Na_2CO_3$-$H_2O$ system. SPS lowers the MSZW and induction time while both parameters were increased in the presence of CMC and PAA. The nucleation inhibition effects were observed to be prominent for both PAA and CMC resulting in observed finer PSDs as cooling rate, *b* increases from 0.5 K/min to 2.65 K/min. The PSD increases with *b* for both pure and SPS additive, whereas they decrease for both PAA and CMC.

## | KEYWORDS

Nucleation and growth kinetics; Metastable zone width; Sodium bicarbonate; Induction time

## | ARTICLE INFORMATION

**ACCEPTED:** 01 December 2022 **PUBLISHED:** 11 December 2022 **DOI:** 10.32996/bjps.2022.2.1.2

## 1. Introduction

Sodium bicarbonate ($NaHCO_3$) is an essential green inorganic chemical widely used in various industries. $NaHCO_3$ is produced by passing $CO_2$ into an aqueous solution to precipitate $NaHCO_3$. Small needle-like $NaHCO_3$ crystals (prone to agglomeration) are obtained [Kang,, 2021, Jiang, 2019]. The addition of $Na_2CO_3$ to a solution of $NaHCO_3$ promotes its crystal growth, size and nucleation [Jiang, 2019]. The particle size distribution (PSD) of substances is important to their transportation and packaging. The crystal nucleation kinetics (measured from the metastable zone width (MSZW) and/or from the induction time) can be obtained from various model adaptations of the CNT and are vital to the control of final crystal properties such as the PSD [Shiau, 2021; Sangwal, 2010; Kashchiev, 2010; Małysiak, 2021].

In the present work, the effect of three polyelectrolyte additives on the nucleation parameters, and PSD of $NaHCO_3$-$Na_2CO_3$ system was investigated. The Nyvlt and Sangwal approaches were used to estimate the nucleation kinetics parameters of $NaHCO_3$-$Na_2CO_3$ from MSZW and induction time data.

### *1.1 Theories for the MSZW*

The MSZW ($\Delta T_m$) denotes the temperature difference between the saturation temperature ($T_0$) and the temperature at which nucleation is detected, ($T_m$) for a given *b*; i.e., $\Delta T_m = T_0 - T_m$. The Nyvlt's model and its modification by Sangwal are two of the most important models for studying the nucleation kinetics by fitting MSZW data against the cooling rates based on CNT. While the Nyvlt's model indicates a linear relationship between $\ln(\Delta T_m)$ vs $\ln b$, the Sangwal's modification, called the self-consistent Nyvlt-like approach proposes a relationship between $\left(\frac{\Delta T_m}{T_0}\right)$ vs *b*. Both models and can used to fit accurately the additive effects on MSZW data. The nucleation order, *m* (which is an indication of the nucleation/growth mechanism) can be obtained from the slope of the models.

Eqs. (1) depicts the Sangwal's self-consistent Nyvlt-like model [Ma, 2009; Li, 2019].

$$\left(\frac{\Delta T_m}{T_0}\right) = \left(\frac{f}{KT_0}\right)^{\frac{1}{m}} \left(\frac{\Delta H}{RT_m}\right)^{\frac{1-m}{m}} b^{\frac{1}{m}} \quad (1)$$

where the slope in Eq. (1) = 1/*m*, and *m* is the apparent nucleation order, *K* is the nucleation constant. Both *m* and *K* are related to the appearance of visible crystals at $T_m$.

Eq. (1) can be expressed in linear form;

$$ln\left(\frac{\Delta T_m}{T_0}\right) = \Phi' - \beta lnT_0 + \beta lnb = \Phi + \beta lnb \quad (2)$$

A plot of $ln\left(\frac{\Delta T_m}{T_0}\right)$ vs *lnb* enables the determination of the value of *m* from the inverse of the slope, $1/\beta$ [10, 11].

## 2. Materials and Methods

Cooling crystallization experiments were conducted in a 300 mL double-jacketed glass vessel using a programmable temperature bath. Pure analytical grade $NaHCO_3$, $Na_2CO_3$ and the polyelectrolye additives were purchased from Sinopharm Chemical Reagent Co. Ltd. and Zichuan Yaodong Chemical Co. Ltd, respectively. 18g of $NaHCO_3$ + 0.4 mol $Na_2CO_3$ were added to a jacketed vessel with 100 g water. The procedure was repeated with water + 10 ppm each of 3 different polyelectrolye additives, sodium polysterene sulfonate (SPS), Polyacetic acid (PAA) and sodium carboxymethylcellulose (CMC). The solutions were heated and stirred at 400 rpm to achieve complete dissolution of all solutes and cooled at varying cooling rates (0.5-2.67 K/min)) from 361.15 K to 308.15 K. The particle size distribution (PSD) was examined by a microscope and ImageJ.

## 3. Results and Discussion

### *3.1 Effect of additive and cooling rates on MSZW*

The existence of three polyelectrolyte additives showed varying effects on the MSZW of $NaHCO_3$-$Na_2CO_3$ system. The MSZW data is listed in Table 1 and fitted to the Sangwal's self-consistent Nyvlt-like model in Figure 1. From Table 1, it can be observed that whilst SPS lowers the MSZW, both CMC and PAA raise it, in the order SPS < Pure < CMC < PAA. Likewise, the trend in MSZW correlates with the nucleation temperatures, $T_o$ (Figure 2), which can be seen to decrease with increasing cooling rates for all measured systems.

The nucleation kinetics of $NaHCO_3$-$Na_2CO_3$ system was studied according to the effects of cooling rate and three polyelectrolyte impurities, and the data is listed in Table 1. At the same $T_o$, the MSZW of $NaHCO_3$-$Na_2CO_3$ system increases with the cooling rate, attributable to the temperature gradient $T_o$-$T_m$, which widens as cooling rate increases. That is to say, at a constant $T_o$, increasing the cooling rate results in decreasing $T_m$, a factor that lowers the supersaturation and consequently the temperature at which the appearance of the crystal nucleus is detected thereby making the MSZW to widen. The temperature gradient $T_o$-$T_m$ =$\Delta T_m$ and *b* are also associated with the duration, $t_m$ (referred to as the induction time and calculated as $t_m = \Delta T_m/b$) at which the crystals are detected, from $T_o$ (Table 2). The $t_m$ is associated with the likely growth of critically sized nuclei to visible entities [Sangwal, 2009]. The $t_m$ decreases with increasing *b*, and is also in the order SPS<Pure<CMC<PAA.

Table 1. MSZW of $NaHCO_3$-$Na_2CO_3$ system at a constant $T_o$ = 361.15 K

| *b, K/min* | $\Delta T_m$ | | | |
|---|---|---|---|---|
| | Pure | SPS | CMC | PAA |
| 0.50 | 22.30 | 21.04 | 26.76 | 28.32 |
| 0.706 | 26.75 | 24.22 | 30.37 | 31.15 |
| 1.177 | 28.12 | 26.22 | 34.60 | 36.35 |
| 2.650 | 30.36 | 28.66 | 36.69 | 37.99 |

Table 2. Induction time of $NaHCO_3$-$Na_2CO_3$ system at a constant $T_o$ = 361.15 K

| *b, K/min* | $t_m$ (s) | | | |
|---|---|---|---|---|
| | Pure | SPS | CMC | PAA |
| 0.50 | 2677.07 | 2525.81 | 3212.48 | 3399.75 |
| 0.706 | 2274.65 | 2059.52 | 2582.48 | 2648.80 |
| 1.177 | 1433.23 | 1336.39 | 1763.50 | 1852.70 |
| 2.650 | 687.34 | 648.85 | 830.65 | 860.08 |

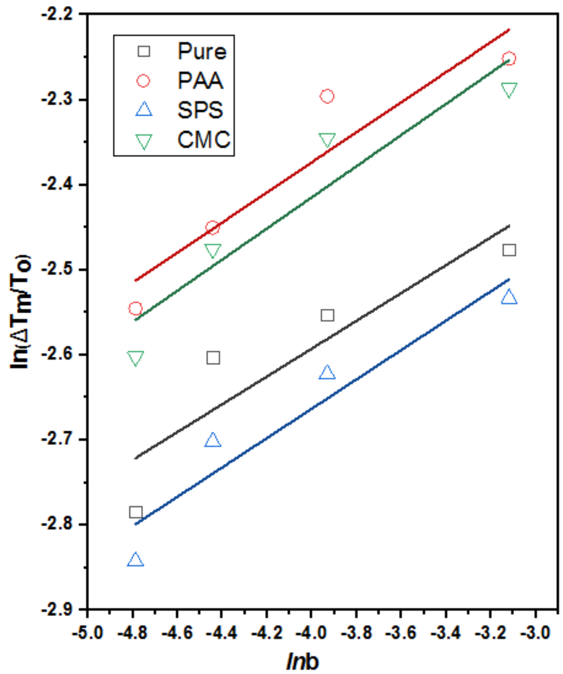


Figure 1. Fitting (solid lines) by the self-consistent Nyvlt-like approach Eq. (3).

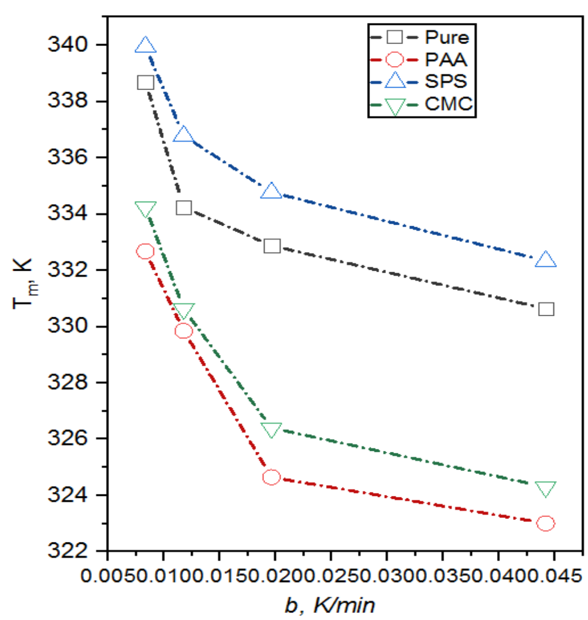


Figure 2. Observed nucleation temperatures indicating the inhibition of nucleation by various additives.

***3.2 Effect of cooling rate on nucleation behaviour***

The introduction of impurities into the crystallizing solution has different effects on the growth mechanism and the interfacial tension of crystals. Table 3 shows the fitting results from Eq. (2). The nucleation order, *m*, values suggest the type of nucleation and growth mechanisms such that $3 < m < 7.5$ depicts progressive nucleation, and $2 < m < 3$ depicts instantaneous nucleation [13]. By fitting the MSZW values of $NaHCO_3$-$Na_2CO_3$ to Eq. (2), the *m* values were; *m*(Pure) = 6.12, *m*(SPS) = 5.80, *m*(PAA) = 5.66, and *m*(CMC) = 5.46. The observed *m* values show that the growth and nucleation mechanism of $NaHCO_3$-$Na_2CO_3$ was by progressive nucleation. Sangwal associated the dimensionless quantity $\Phi$ in Eq. (2) to the adsorption of impurity on the crystal nuclei, which affects the diffusion of solute molecules in the solution [Huang, 2009]. It can be speculated from Table 3 that the diffusion of solute molecules was also impacted to some extent by the additives.

Table 3. Fitting results from Figure 1 and Eq. (2)

| | $\beta$ | $\Phi$ | $m$ | Eq. (2) | $R^2$ |
|---|---|---|---|---|---|
| Pure | 0.16352 | -1.93809 | 6.11546 | $\ln(\Delta T_m/T_o) = 0.16352\ln b - 1.93809$ | 0.8168 |
| CMC | 0.18308 | -1.68199 | 5.46209 | $\ln(\Delta T_m/T_o) = 0.18308\ln b - 1.68199$ | 0.8889 |
| PAA | 0.17666 | -1.66657 | 5.66059 | $\ln(\Delta T_m/T_o) = 0.17666\ln b - 1.66657$ | 0.8832 |
| SPS | 0.17254 | -1.97267 | 5.79575 | $\ln(\Delta T_m/T_o) = 0.17254\ln b - 1.97267$ | 0.9100 |

***3.3 Effect of cooling rate on nucleation behaviour***

$NaHCO_3$ crystals with different morphologies were obtained in water (pure) and in the presence of various additives; needle-like (pure), columnar (SPS), and also flaky (PAA and CMC), at different cooling rates as shown in Figure 3. Varying PSDs were observed as shown in Figure 4; the PSD increases with *b* for both pure and SPS additive, whereas they decrease with *b* for both PAA and CMC. The PSD is highest in the presence of SPS additive. In all cases, a higher *b* corresponds to an observed smaller $T_m$, leading to varying nucleation inhibition effect, PSDs and MSZWs. The nucleation inhibition effect was prominent for both PAA and CMC resulting in observed finer PSDs as *b* increases from 0.5 K/min to 2.65 K/min. However, the opposite is true for pure and SPS systems whereby PSDs and crystal sizes increased with increasing cooling rate. That is to say, at a higher *b*, in both pure and SPS systems, faster nucleation was promoted resulting in larger PSDs with bigger size. The observed PSD and MSZW in the various additives are consistent since the PSD is directly related to MSZW, and a smaller or narrower MSZW is usually associated with an increase in PSD [Huang, 2009].

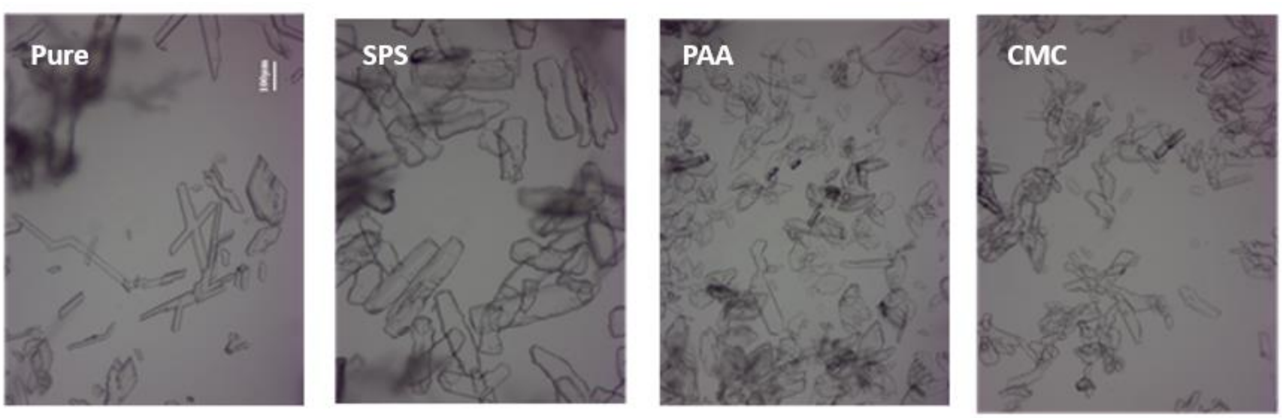


Figure 3. Morphology of $NaHCO_3$-$Na_2CO_3$ in different additives, $b$ = 0.7 K/min, scale = 100 µm

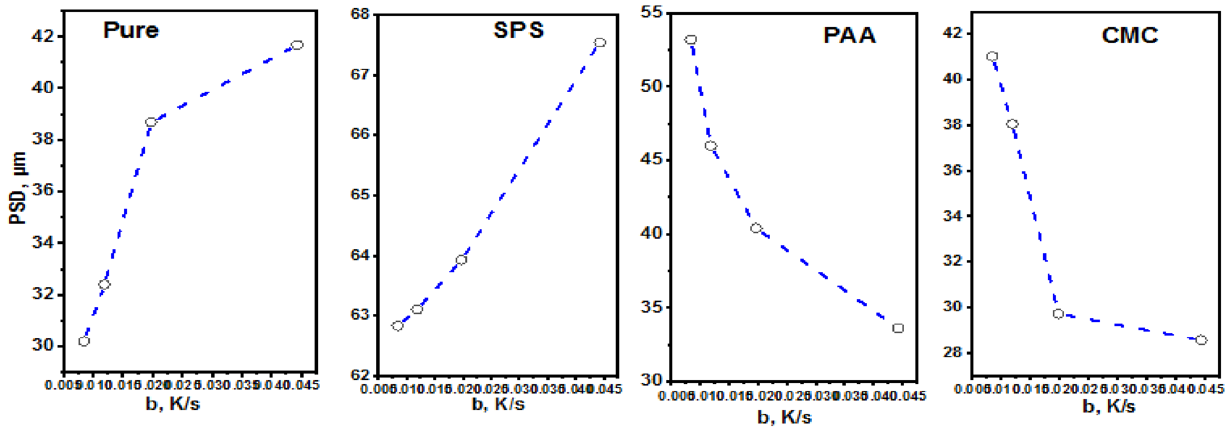


Figure 4. PSD of $NaHCO_3$-$Na_2CO_3$ crystals in different additives

## 4. Conclusion

The effect of three polyelectrolyte additives (sodium polysterene sulfonate (SPS), Polyacetic acid (PAA) and sodium carboxymethylcellulose (CMC)) on the nucleation parameters, and particle size distribution (PSD) of $NaHCO_3$-$Na_2CO_3$ was investigated. By estimating the nucleation kinetics of $NaHCO_3$-$Na_2CO_3$ from the metastable zone width data, it was seen that whilst SPS lowers the MSZW, CMC and PAA raised it in the order SPS < Pure < CMC < PAA. The PSD increases with cooling rate, *b* for both pure and SPS additive, whereas they decrease with *b* for both PAA and CMC. A higher *b* corresponds to an observed smaller nucleation temperature leading to varying nucleation inhibition effect, PSDs and MSZWs. The nucleation inhibition effect was prominent for both PAA and CMC resulting in observed finer PSDs as *b* increases from 0.5 K/min to 2.65 K/min. The results can guide the crystallization of $NaHCO_3$ for improved particle size distribution, transportation and packaging.

**Funding:** This research received no external funding.
**Conflicts of Interest:** The authors declare no conflict of interest.
**Publisher's Note**: All claims expressed in this article are solely those of the authors and do not necessarily represent those of their affiliated organizations, or those of the publisher, the editors and the reviewers.

## References

[1] Jiang, S., Zhang, Y and Li, Z. (2019) A new industrial process of $NaHCO_3$ and its crystallization kinetics by using the common ion effect of $Na_2CO_3$, *Chemical Engineering Journal, 360* 740-49.
[2] Huang, Y., Lu, J., Chen, H., Du, W and Wang, X. (2019). Effects of succinic acid and adipic acid on the metastable width of glutaric acid in acetic acid, *Journal of Crystal Growth, 507* 1-9.
[3] Kang, Z.L, Zhang, X.H., Li, K Li, Y.P., Lu, F. Ma, H.J., Song, Z.J., Zhao, S.M and Zhu M.M (2021). Effects of sodium bicarbonate on the gel properties, water distribution and mobility of low-salt pork batters, LWT, 138 110567.
[4] Kashchiev, D, Borissova, A, Hammond, R.B, and Roberts, K.J. (2010). Effect of cooling rate on the critical undercooling for crystallization, *Journal of Crystal Growth, 312* 698-704.
[5] Li, D, Ma, Y., Meng, L., Guo, Y., Deng, T and Yang, L. (2019). Effect of impurity ions on solubility and metastable zone width of lithium metaborate salts, Crystals, 9 (2019) 182.
[6] Małysiak, A, Orda, S, and Drzazga, M. (2021). Influence of Supersaturation, Temperature and Rotational Speed on Induction Time of Calcium Sulfate Crystallization, Crystals, 11 1236.
[7] Ma, Y, Zhu, J, Ren, H and Chen, K. (2009). Effects of impurity ions on solubility and metastable zone width of phosphoric acid, Crystal Research and Technolology, 44 1313-18.
[8] Shiau, L.D (2021). Comparison of the Nucleation Parameters of Aqueous l-glycine Solutions in the Presence of l-arginine from Induction Time and Metastable-Zone-Width Data, Crystals, 11 1226.
[9] Shiau, L.D, and Lu, T.S. (2014). A model for determination of the interfacial energy from the induction time or metastable zone width data based on turbidity measurements, CrystEngComm, 16 9743-52.
[10] Sangwal K. (2010). On the effect of impurities on the metastable zone width of phosphoric acid, *Journal of Crystal Growth, 312* 3316-25.
[11] Sangwal, K. (2009). Effect of impurities on the metastable zone width of solute–solvent systems, *Journal of Crystal Growth, 311* 4050-61.
[12] Sangwal, K. (2009). Novel approach to analyze metastable zone width determined by the polythermal method: physical interpretation of various parameters, *Journal of Crystal Growth, 9* 942-50.
[13] Sangwal, K. (2009). A novel self-consistent Nývlt-like equation for metastable zone width determined by the polythermal method, *Crystal Research and Technolology, 44* 231-47.
[14] Xu, S., Zhang, H., Qiao, B and Wang, Y. (2021). Insights into solvent-dependent nucleation behavior of benzoic acid from metastable zone widths, *Journal of Molecular Liquids, 343* 117634.